

Fluorescence correlation spectroscopy of CdSe/ZnS quantum dot optical bioimaging probes with ultra-thin biocompatible coatings

Michael J. Murcia, David L. Shaw, Eric C. Long*, Christoph A. Naumann*

Department of Chemistry and Chemical Biology, Purdue School of Science, Indiana University-Purdue University Indianapolis (IUPUI),
402 North Blackford Street, Indianapolis, IN 46202, USA

Received 19 June 2007; accepted 30 July 2007

Abstract

The colloidal stabilities and emission properties of CdSe/ZnS quantum dot (QD) optical probes capped with a variety of thin, hydrophilic surface coatings were studied using confocal fluorescence correlation spectroscopy. These coatings are based on mercaptoethanol, mercaptopropionic acid (with and without conjugated aminoethoxyethanol), lipopolymers (DSPE-PEG2000), cysteine (Cys), and a variety of Xaa-Cys dipeptides. The study shows that QDs with thin hydrophilic coatings can be designed that combine good colloidal stability and excellent emission properties (brightness). Furthermore, there is a general correlation between colloidal stability and brightness. The experiments reported illustrate that QDs with multiple types of thin coatings can be created for optical imaging applications in a biological environment while also maintaining a size below 10 nm.

© 2007 Elsevier B.V. All rights reserved.

Keywords: CdSe/ZnS quantum dots; FCS

1. Introduction

Current advances in the life sciences are linked to the availability of sophisticated new experimental tools to enable the manipulation of biomolecules and the study of biological processes at the cellular and molecular levels. Central to the above, fluorescent optical probes are fundamental to furthering our understanding of the structure, organization, and dynamic properties of biological systems under *in vivo* conditions. While traditional fluorescent probes are μm -size colloidal particles and dye molecules that have limited performance due to either their relatively large sizes or poor photo-stabilities, more recently new classes of imaging probes based on nanometer-sized photo-luminescent nanoparticles have emerged that exhibit

highly attractive photophysical properties [1,2]. Among these, semiconductor nanoparticles, known as quantum dots (QDs), represent a particularly prominent class of nanoparticle imaging agents [3–7]. Unlike organic dye probes, QDs are characterized by large Stokes shifts, broad absorption bands, and narrow, size-dependent emission bands without a significant red tail [3–7]. In addition, the unique absorption and *size-dependent* emission properties of nanoparticles are very beneficial for multi-color experiments because multiple color QDs can be excited using a single laser excitation wavelength. Finally, unlike many nanoparticle-based optical imaging probes employed in previous studies, QDs do not exceed the size of proteins.

The size-dependent emission of QDs is the result of a quantum confinement effect, which occurs when the size of the exciton (given by the exciton Bohr radius, r_{Bohr}) exceeds the physical size of the semiconductor nanocrystal (D) [8]. Semiconductor nanocrystals exhibit particularly interesting properties when the exciton is strongly confined

* Corresponding authors. Fax: +1 317 274 4701.

E-mail addresses: long@chem.iupui.edu (E.C. Long), naumann@chem.iupui.edu (C.A. Naumann).

($D < 2r_{\text{Bohr}}$) [9] and outperform fluorescent dyes in terms of brightness and photostability [10]. These additional features make quantum dots particularly attractive for quantitative, long-term observations of dynamic biological processes. Interestingly, QDs can also be synthesized with emission bands in the near infrared (NIR) wavelength range. Such NIR QDs are particularly attractive for *in vivo* animal imaging applications [11,12].

In optical imaging applications, the development of ZnS-shelled CdSe QDs (i.e., CdSe/ZnS QDs) has received considerable attention because their narrow emission bands span the whole optical spectrum. Originally, the synthesis of CdSe QDs was challenging because it entailed the heating of pyrophoric precursors such as $\text{Cd}(\text{CH}_3)_2$ and elemental Se in trioctylphosphine (TOP)/trioctylphosphine oxide (TOPO) at reaction temperatures of 250–350 °C for 24 h, followed by a size-selective precipitation [3,13]. Therefore, efforts have been made recently to improve and simplify the synthesis procedure. For example, Peng and coworkers showed that Cd-containing QDs can be formed by thermal means from non-pyrophoric precursors, such as CdO and $\text{Cd}(\text{OAc})_2$ [6,14]. In addition, a facile sonochemical synthesis procedure for highly-luminescent CdSe/ZnS QDs has been developed recently by our Groups [15]: By adapting the use of $\text{Cd}(\text{OAc})_2$, TOPO and hexadecylamine (HDA) to an ultrasound-driven reaction and by pursuing a subsequent sonochemical ZnS shelling procedure using Zn-ethylxanthate, highly luminescent CdSe/ZnS QDs with quantum yields of 50–60% can be obtained. As shown in Fig. 1, the sonochemically-synthesized QDs show broad absorbance and narrow emission bands in their spectra; successful shelling can be confirmed spectroscopically through the observation of an emission increase and structurally by direct high-resolution transmission electron microscopy (HRTEM) imaging (Fig. 1) of the size of CdSe *vs.* CdSe/ZnS QDs.

Unfortunately, QDs are not water-soluble upon completion of their synthesis. Therefore, to be suitable for biological imaging applications, QDs need to be rendered water-soluble and also need to be biocompatible. To achieve biocompatibility, the protective coatings of a QD should lead to the following properties: (i) colloidal stability (i.e., a lack of aggregation) in a biological environment; (ii) no significant non-specific surface adsorption of biomolecules; and (iii) low cytotoxicity. Indeed, QD coating strategies such as those based on hydrophilic polymers like poly(ethylene glycol) (PEG) [16], polyelectrolytes [17], proteins [18,19], PEG-lipids [20], polysaccharides [21], and peptides [22] have allowed the successful application of CdSe/ZnS QDs to imaging in cell cultures and in live animals. Although effective, most coatings employed so far have been relatively thick, thus leading to capped QDs of more than 20 nm in size. However, label size is often a critical parameter in many imaging applications. Therefore, the goal of the current study was to explore a variety of potential QD imaging probes with thin, biocompatible coatings that maintain the overall probe size below 10 nm.

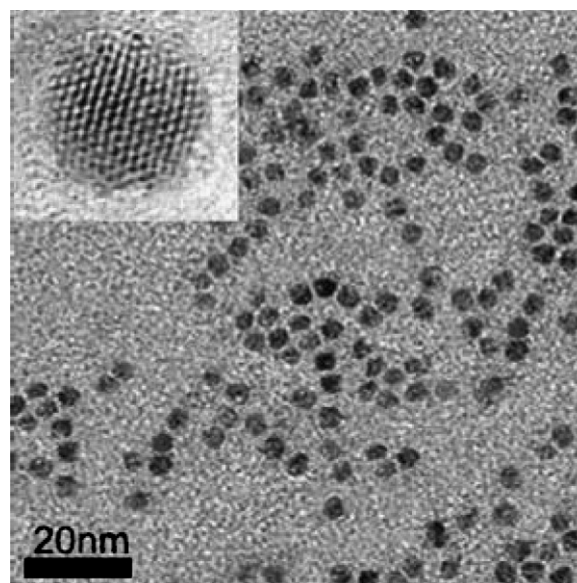
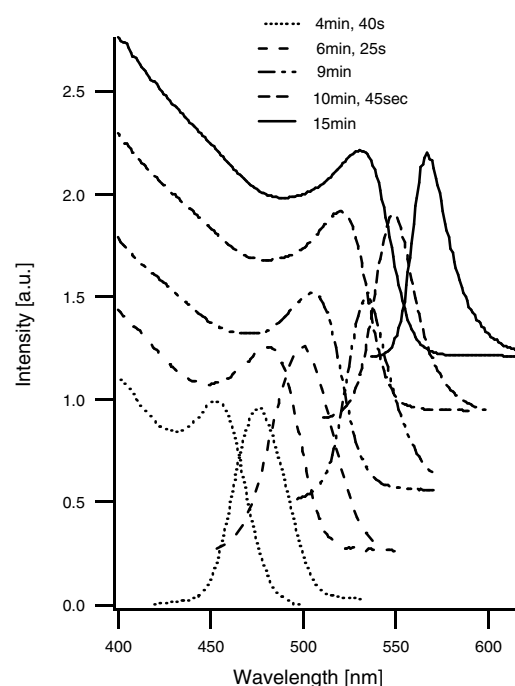


Fig. 1. Absorbance and emission spectra (upper panel) and TEM micrograph (lower panel) of sonochemically synthesized CdSe/ZnS QDs. The spectral shift illustrated in the upper panel is associated with increasing sonication time. The high crystallinity of the QDs is illustrated in the inset as obtained via HRTEM (size of the inset is 5.4 nm × 5.1 nm) [15].

Considering surface coatings further, it is generally accepted that biocompatibility is best achieved when surfaces are electrically neutral, hydrophilic and highly dynamic [23]. A paradigm of such a biocompatible surface is a solid substrate surface-functionalized with poly(ethyleneglycol) (PEG). In this case, surface resistance to adsorption occurs through the steric repulsion of proteins by grafted PEG chains [24–26] and increasing the density and thickness of a polymer coating is consid-

ered to improve biocompatibility. Interestingly, coatings with very short grafted oligomers, such as PEG of only two ethylene oxide segments, also were found to prevent protein adsorption efficiently [27,28]. This finding was supported by single-chain mean field theory calculations that highlighted the importance of blocking possible protein binding sites on the solid substrate to achieve a biocompatible surface design [29]. These experimental and theoretical findings suggest that ultrathin biocompatible coatings can be designed as long as these coatings lower the surface energy of the solid substrates by high surface coverage (high grafting density). Importantly, the above considerations provide a rationale for the current study: By exploring the colloidal stability and photophysical properties of QDs with thin hydrophilic surface coatings, *this study seeks to provide insight into their applicability for optical imaging applications in a biological milieu*. Thus a main goal of the current approach is to design small, biocompatible QDs of less than 10 nm in diameter.

Nanoparticles should also remain monodisperse in a biological environment to be biocompatible. Therefore, an important first step in evaluating a new surface coating is to explore the colloidal stability of surface capped QDs in an aqueous environment. Traditionally, the size and size distribution of nanoparticles has been studied using TEM and dynamic light scattering (DLS) [30–35]. More recently, fluorescence correlation spectroscopy (FCS) has emerged as an interesting alternative to these methods to study the size and diffusion properties of fluorescent nanoparticles. For example, FCS was used successfully to explore the size and diffusion properties of Si nanoparticles and QDs [36–38] and was successfully applied to verify the monodispersity of hydrophobic nanocrystals in an aqueous environment after capping with amphiphilic polymers [37]. Unlike TEM or DLS, FCS also provides information about the photophysical properties of photoluminescent nanoparticles, such as the photon count rate. The ability to study photophysical properties is a particularly attractive feature for the study of QDs because it is known that the quality of a QD coating not only affects the colloidal stability of these nanocrystals, but also their emission properties and photostabilities.

The goal of the current study was to explore the colloidal stabilities and the emission properties of CdSe/ZnS QDs capped with a variety of ultra-thin coatings (Fig. 2) using confocal FCS; we show that FCS can be applied successfully to evaluate the quality of these capped nanocrystals. In an effort to minimize the nanoparticle coating thickness, several test coatings were chosen initially for investigation: mercaptoethanol (ME), mercaptopropionic acid (MPA), MPA-conjugated 2,2-(aminoethoxy) ethanol (MPA/AEE), and a lipopolymer encapsulated system. While ME and MPA were used as direct surface exchange coatings to replace the hydrophobic coordinating solvents and AEE was employed as a secondary layer covalently conjugated to an initial mercaptopropionic acid (MPA)

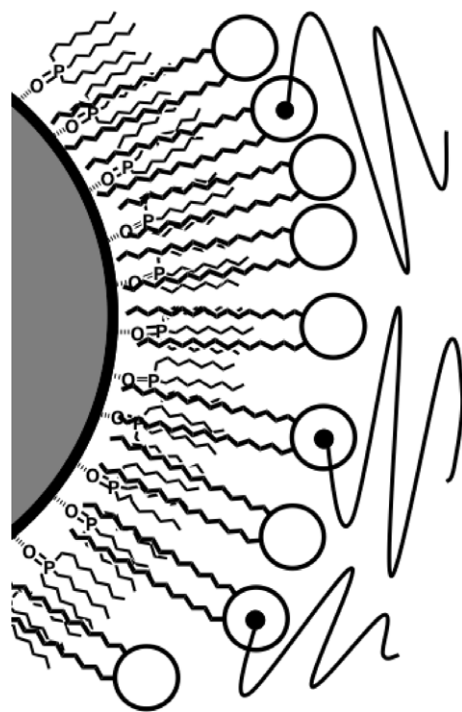
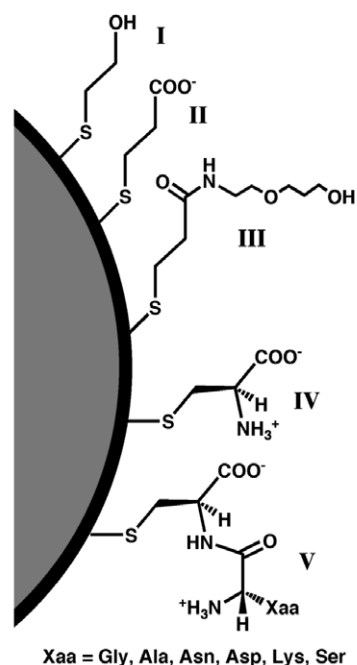


Fig. 2. Illustration of the variety of ultrathin QD surface coatings analyzed in this study. Surface exchange coatings (upper panel): 2-mercaptoethanol (ME, I); mercaptopropionic acid (MPA, II); *N*-(2-(2-hydroxyethoxy)ethyl)-3-mercaptopropionamide (MPA/AEE, III); Cys (IV); and Xaa-Cys (where Xaa is Gly, Asp, Asn, Ala, Lys, or Ser, V); the lipopolymer encapsulated system (lower panel) consists of 40% 1,2-dipalmitoyl-*sn*-glycero-3-phosphoethanolamine-*N*-mPEG-200 (illustrated as lipids with a black dot) and 60% 1,2-dipalmitoylglycero-3-phosphocholine.

coating (via EDC-catalyzed amide bond formation), the lipopolymer encapsulated system [20] makes use of the

hydrophobicity of the coordinating solvent to enable the encapsulation of the entire QD. Further, several coatings were investigated based on the amino acid cysteine (Cys) and Cys-containing dipeptides. Amino acids and dipeptide coatings [39] based on Cys provide a side chain sulfhydryl for their attachment to the QD surface similar to the thiols provided by ME and MPA. These particular ultrathin coatings thus enable the investigation and exploitation of the chemical diversity provided by amino acids and therefore a determination of the influence of basic, acidic, neutral, and polar functionalities on the colloidal stability of CdSe/ZnS QDs in a peptide environment of uniform length. Importantly, such coatings also enable the final QD formed to closely resemble protein-based materials perhaps increasing their overall biocompatibility and biological targeting capabilities.

2. Confocal fluorescence correlation spectroscopy

Confocal fluorescence correlation spectroscopy, or FCS, is a powerful tool that can be applied to the analysis of quantum dots [37,38]. FCS is based upon the fluctuating fluorescence signal of a fluorophore as it passes through a confocal excitation volume that is on the order of a femtoliter (10^{-15} L) [40–44]; fluorescence emission intensities can be monitored over time with avalanche photodiodes and sent to a computer for analysis where the intensity fluctuation is translated into the autocorrelation function shown in Eq. (1):

$$G(\tau) = 1 + \frac{\langle \delta I(t) \delta I(t + \tau) \rangle}{\langle I(t) \rangle^2} \quad (1)$$

As outlined in Eq. (1), the fluorescence fluctuation from the average intensity, $\delta I(t)$, is monitored and correlated to the fluctuation at time $t + \tau$ to generate an autocorrelation function. By setting Eq. (1) equal to the autocorrelation function for a 3D Gaussian volume (Eq. (2)), as in the case of the confocal excitation volume, valuable information about the average diffusion time and concentration of molecules and the average intensity per molecule can be extracted.

$$G(\tau) = 1 + \frac{1}{N} \left(1 + \frac{\tau}{\tau_D} \right)^{-1} \left(1 + S^2 \cdot \frac{\tau}{\tau_D} \right)^{-\frac{1}{2}} \quad (2)$$

In Eq. (2) above, N is the number of fluorophores in the confocal volume at any time, τ_D is the time a molecule takes to diffuse through the confocal volume, and S is a structure parameter for the confocal volume equal to the width/height. To maximize the intensity fluctuations, and therefore the signal, it is critical that the concentration of fluorophores be very low so the intensity change is greatest when a fluorescent molecule enters or exits the confocal volume. This inverse relationship between the number of fluorescent molecules and signal can clearly be seen in Eq. (2), and translates to operating concentrations in the nanomolar range.

Knowing the number of fluorophores in the confocal volume and the overall emission intensity, the intensity per fluorophore can be calculated. With this method of measuring emission intensity per QD, FCS can evaluate and compare readily the impact of a designed surface coating on the fluorescence intensity at the single QD level. Indeed, using a determined diffusion time, it is possible to calculate the hydrodynamic radius (r) of the fluorophore using the Stokes–Einstein relationship shown in Eq. (3):

$$r = \frac{2\tau_D \cdot k \cdot T}{3\pi \cdot \eta \cdot \omega^2} \quad (3)$$

where ω is equal to the radius of the confocal volume, τ_D is the diffusion time, η is viscosity, and k is the Boltzmann constant. By monitoring the nanoparticle size and concentration over time, it is therefore possible to evaluate the ability of a nanoparticle surface coating to prevent aggregation.

3. Experimental design and methods

3.1. Synthesis of CdSe/ZnS core/shell QDs

CdSe/ZnS core/shell QDs were synthesized sonochemically [15]. The approach of Peng and coworkers [6,14] was adapted to the ultrasound synthesis of TOPO-coated CdSe quantum dots using hexadecylamine (HDA), Cd(OAc)₂, and TOPO. HDA was chosen as a capping agent because it was reported to result in high-quality quantum dots, but octadecylamine (ODA) can also be substituted [45]. In all cases, the Cd:Se ratio was held at 1:5, and the overall Cd concentration in the coordinating solvent was 0.33 mol/kg. A typical synthesis was carried out as follows: TOP and selenium powder were placed in a side arm test tube purged continuously with argon (note that nitrogen is not an inert atmosphere when sonication is used [46]). The selenium powder was dissolved by sonicating for 2 min using a high energy sonifier (Branson, Model 450) equipped with a micro-tip operated at a frequency of 20 kHz and an ultrasonic power of 9–10 W. Subsequently, Cd(OAc)₂, TOPO, and stearic acid (60:40 TOPO:SA) or Cd(OAc)₂, TOPO, and HDA (75:25 TOPO:HDA) [47] were placed in identical Ar-purged reaction vessels. These reactants were heated gently to melt the mixture, and the previously-prepared Se/TOP solution was injected into the melt. At that time, sonication was initiated using a specific ultrasonic power (in the range of 9–30 W; frequency: 20 kHz) chosen so as to effect the desired reaction kinetics, and product aliquots were taken as the reaction color was observed to change from pale yellow to deep red. All aliquots were washed (3×5 mL) with acetone/methanol and dried under high vacuum. Before use, the product material was dispersed in dry chloroform and centrifuged to sediment any remaining particulate matter.

ZnS shell formation over the CdSe cores generated as described above was carried out using zinc ethylxanthate synthesized via the procedure of Ikeda and Hagihara [48].

The zinc nitrate hexahydrate and potassium ethylxanthate used in this preparation, as well as tributylphosphine (TBP) were purchased from Aldrich and used without further purification. To obtain ZnS-shelled quantum dots, aliquots of freshly synthesized CdSe core material in coordinating solvent (4 mL) were placed into a separate reaction vessel. Zinc ethylxanthate (0.10 g, 0.53 mmol) was then dissolved in TBP (2.0 mL, 8.1 mmol) and added to the 4 mL aliquot of CdSe core solution. Facilitating their synthesis, purification of core CdSe nanoparticles prior to the addition of the ZnS shell was not found to be necessary.

3.2. Preparation of mercaptopropionic acid (MPA), mercaptoethanol (ME), aminoethoxyethanol (AEE), and lipopolymer coated CdSe/ZnS core/shell QDs

The first approach to hydrophilic surface modification of the nanocrystals was a surface exchange of the hydrophilic coordinating solvent with commonly used hydrophilic thiol acids such as mercaptopropionic acid (MPA) or mercaptoethanol (ME) [49,50]. The procedure for this reaction involved washing away any excess coordinating solvent from the CdSe/ZnS nanocrystals and placing them in the presence of an excess of the replacement coating. The weakly bound coordinating solvent is a labile coating easily replaced with the more tightly binding mercapto-acid by stirring in chloroform for 24 h. Specifically, 0.5 g of the crude, shelled QD sample was washed and precipitated 3× with a solution of 50/50 methanol/acetone and dissolved in 12 mL of chloroform containing 0.25 g of MPA. This solution was stirred under argon for 24 h, at which time the hydrophilic nanocrystals precipitate from the chloroform. The solution was then centrifuged to separate the hydrophilic nanocrystals, and the sediment washed in hexane (3×). The dry product was then placed under vacuum to remove excess organic solvent, and subsequently dispersed in water. This procedure has been used extensively and the exchange from coordinating solvent to a hydrophilic thiol coating has been shown to be effective by NMR [51]. To form AEE-coated QDs, the primary amine of amino diethylene oxide was reacted with MPA-coated QDs using standard EDC coupling chemistry.

The second hydrophilic modification approach retained the hydrophobic coordinating solvent and added amphiphilic lipids and lipopolymers to encapsulate the hydrophobic QDs. This somewhat thicker lipopolymer coating was employed as a positive control in our studies because it has proven to be a viable bioinert QD coating [20]. As illustrated in Fig. 2, hydrophobic forces cause the acyl chains of the amphiphilic lipids and lipopolymers to pack with the hydrophobic nanoparticle surface giving it a biologically inert polymer coating in an aqueous environment; this approach was first reported by Dubertret and coworkers [20]. Quantum dots (0.5 g of the crude, shelled QDs) were washed as in the surface exchange method to remove any excess coordinating solvent. The hydrophobic nanoparticles were then re-dispersed in a chloroform solution containing

5.5 μmoles of 40% 1,2-dipalmitoyl-*sn*-glycero-3-phosphoethanolamine-*N*-[methoxy(polyethyleneglycol)-2000] (mPEG-2000 PE) and 60% 1,2-dipalmitoylglycero-3-phosphocholine (DPPC). After the chloroform completely evaporated, the residue was heated to 80 °C followed by the addition of 1 mL of distilled water, resulting in an optically transparent solution of lipopolymer-encapsulated QDs. One advantage of this technique compared to the surface exchange method is the reduced chance for nanoparticle surface degradation since the bare nanoparticle is not exposed during the coating procedure.

3.3. Preparation of Cys and Cys-dipeptide coated CdSe/ZnS core/shell QDs

3.3.1. Peptide synthesis

Fmoc derivatized amino acids and solid support resins were purchased from Bachem. All other chemical reagents were purchased from Sigma–Aldrich or other commercial sources. Commercial reagents were used without further purification unless otherwise stated. Peptides were synthesized using standard manual solid-phase Fmoc protocols and commercially-available Fmoc-protected amino acid derivatives on 4-(2',4'-dimethoxyphenyl)-Fmoc-amino-methyl)phenoxy (Rink amide) resin for syntheses leading to carboxy-terminal peptide amides upon final deprotection. Alternatively, substituted 2-chlorotrityl resins were used to generate carboxy-terminal dipeptide acids. Peptide purities and identities were verified by LC–MS using an Agilent Series 1100 LC–MS.

3.3.2. QD surface substitution

In a typical preparation of amino acid- or peptide-coated core/shell QDs, 250 μL stocks of freshly prepared core/shell nanocrystals in coordinating solvent were vortexed once in a 1:1 acetone:methanol solution to remove excess coordinating solvent. These solutions were then centrifuged to sediment the nanocrystalline product that was subsequently dispersed in a small volume (~1 mL) of chloroform. Depending upon the desired batch size, 100–200 μL aliquots of these chloroform solvated nanocrystals were removed and placed in a reaction vessel along with a magnetic stir bar. Subsequently, an excess of the desired surface coating (MPA, Cys, or Cys-dipeptide) was dissolved in 2 mL of NaOH-saturated methanol (basified methanol) and then added to the nanocrystal solution suspended in chloroform. After stirring for several hours (or overnight), the cloudy basified methanol/chloroform nanocrystal solution was centrifuged. The sediment was washed with basified methanol, centrifuged again, and dried under vacuum; most of these materials were now found to be soluble in aqueous media. Upon drying, 150 mM phosphate buffer, pH 9, was then added and vortex mixed until the nanocrystal sediment was re-suspended in solution. These resulting aqueous solutions of nanocrystals were again centrifuged to remove any large aggregates and filtered through 0.2 μm (PP) Whatman syringe filters into final collection vessels for further analyses.

3.4. FCS analysis

Fluorescence correlation spectroscopy was conducted using a Confocor 2 two-channel Fluorescence Correlation Spectrometer system (Carl Zeiss, Inc.) that included the stage of an inverted microscope (Axiovert 200M), a laser excitation module, and an avalanche photodiode (APD)-based detection unit [52]. QDs were excited at 488 nm using an Ar ion laser. The laser light was focused to a diffraction-limited spot using a water immersion objective (C-Apochromat, 40 X, 1.2 Corr). The fluorescence signal was detected using one of the two APDs of the FCS detection unit after passing through a long pass filter (LP 530 nm). To study the colloidal and photo stabilities of QDs, the time fluctuation of the fluorescence intensity was further analyzed using a software correlator. The autocorrelation curve generated by the fluorescent nanoparticles diffusing in bulk solution through a confocal excitation volume was used to calculate the average time necessary for a molecule to pass through the confocal volume, τ_D and the average photon counts per molecule. Using the diffusion time and the radius of a calibrated confocal volume, the hydrodynamic radii of each QD sample could be obtained using the Stokes–Einstein relationship (Eq. (3)). The diffusion time of a dye with a known diffusion coefficient can be measured and applied to Eq. (4) to determine the size of the confocal volume.

$$\tau_D = \frac{\omega^2}{4D} \quad (4)$$

By utilizing this technique to monitor the hydrodynamic radius and the counts per molecule over time, it was possible to evaluate the ability of a newly designed surface coating to prevent nanoparticle aggregation. Autocorrelation curves generated by nanoparticle solutions of equal concentration were used also to calculate the average particle diameter over time.

4. Results and discussion

4.1. Non-peptide-based ultrathin QD coatings

4.1.1. Colloidal stability

FCS analyses [37,38] of ME, MPA, MPA-conjugated AEE (MPA/AEE), and lipopolymer encapsulated CdSe/ZnS QDs led to the autocorrelation curves shown in Fig. 3. For comparison, the diffusion of rhodamine dye was measured in parallel. All QDs used for this study exhibited emission maxima at 570 nm and were from the same QD core/shell synthetic preparation. As a result, the particle size distribution among these samples was <10%, as verified by TEM/HRTEM. All measurements were performed in 0.1 M PBS, pH 7, buffer solutions immediately after the core/shell nanoparticles underwent hydrophilic surface modifications. The actual time between dispersing the nanoparticles in buffer and performing the first measurements was approximately 10 min.

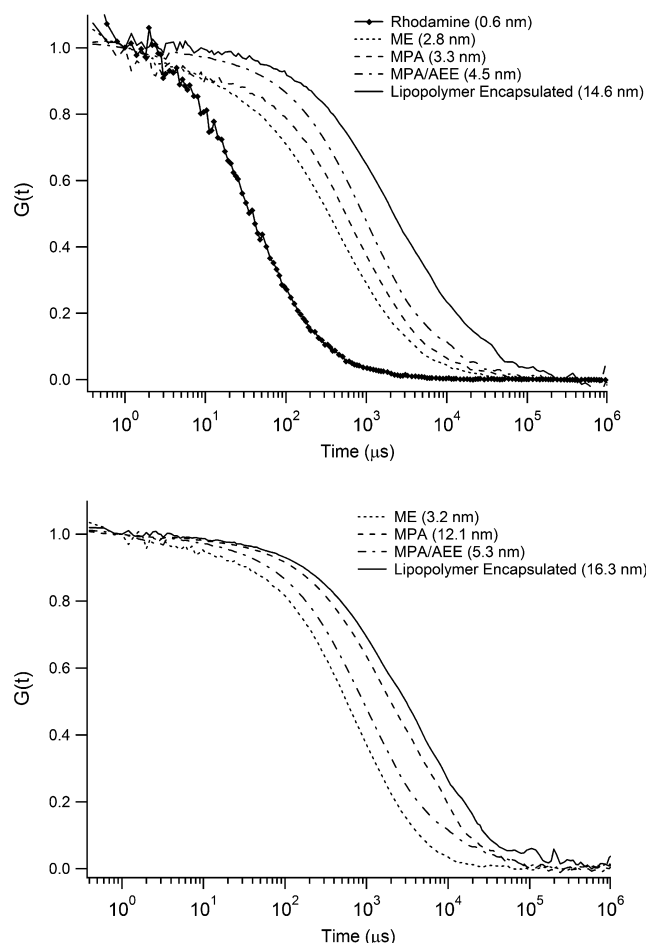


Fig. 3. FCS analyses of ME, MPA, MPA-conjugated AEE (MPA/AEE), and lipopolymer-encapsulated CdSe/ZnS QDs in 0.1 M PBS buffer, pH 7.0. FCS analysis immediately ($t = 10$ min) after sample preparation (upper panel); FCS analysis of colloidal stability after one week of incubation (lower panel).

To evaluate the monodispersities of the different QD samples, the diffusion times of the nanoparticles, calculated from the inflection point of their respective autocorrelation curves shown in Fig. 3, were used to determine the hydrodynamic radius of each nanoparticle by the Stokes–Einstein relationship outlined in Eq. (3). Larger nanoparticles move more slowly, and therefore take longer to pass through a set volume. Through the use of this technique, the particle sizes of the four hydrophilic nanoparticles were measured. The ME coating was the thinnest coating used in this study, as reflected by ME coated QDs having the smallest measured particle diameter, 2.8 nm. By adding a thin AEE layer to the MPA coated nanocrystals, the overall particle diameter increased by 1.2 nm over the 3.3 nm MPA QDs. The relatively large PEG lipopolymer coating showed a measured size of 14.6 nm. It should be noted that efforts towards reducing the size of the lipopolymer were also made by using shorter PEG lipopolymers (350 and 750 MW); however, these systems failed to produce stable, hydrophilic nanoparticles. A likely cause for this instability is the highly curved nature of

the QD surface that requires an amphiphile with a relatively small hydrophobic and large hydrophilic region to cover the entire nanoparticle surface. By decreasing the size of the hydrophilic polymer, it is possible that portions of the hydrophobic coordinating solvent were exposed, which would likely cause the nanoparticles to aggregate in an aqueous environment.

To evaluate the colloidal stability of these coatings as a function of time, FCS measurements on the above samples were repeated a week later, with the results shown in Fig. 3, lower panel (data were collected 10 min after completion of sample preparation). While aggregation of charged quantum dots from charge shielding should occur within hours, the duration of one week was chosen to give ample opportunity for the uncharged quantum dot coatings to reveal any instability. It was observed that although the thin ME coating is only one ethylene glycol “monomer” in length, it was surprisingly effective at preventing nanoparticle aggregation. The loss of colloidal stability due to charge screening is demonstrated by charged MPA coated QDs having an increased diffusion time in the FCS measurement. The AEE coated nanocrystals, although having the same base layer as the MPA coated QDs, demonstrated a resistance to aggregation similar to the ME coating. Surprisingly, the increase in particle diameter of the thin ethylene oxide coatings was not notably greater than the increase for the larger, PEG2000 lipopolymer encapsulated QDs. This implies that under the conditions used only a very short ethylene glycol layer is needed to inhibit aggregation. The good colloidal stability observed for QDs with the ME and the ME/AEE coatings is surprising [53] because these coatings are based on the rather labile coupling of monothiol to the QD surface.

4.1.2. Emission properties

In addition to providing size information through diffusion times, FCS is a single molecule fluorescence technique capable of providing data about the emission intensities of individual nanoparticles. As a result, FCS is a useful tool in evaluating the effects of nanoparticle coatings on photoluminescence properties. Using the same excitation power, the fluorescence intensity, in terms of emission counts per molecule, was measured for each sample and summarized in Table 1. In general, the surface-exchanged coatings were observed to lead to decreased nanoparticle emission intensities when compared to the lipopolymer encapsulated

QDs; each surface-exchanged thin coating exhibited a different extent of decreased emission efficiency, with the AEE coated nanoparticles having the brightest sustainable emission, and the ME coated QDs showing the greatest diminution in intensity. These decreases in intensity may be a function of the hydrophilic coatings trapping excited electrons, similar to how nanocrystal surface defects lead to non-radiative relaxation of an excited state. The reduced emission using thin coatings may also result from a thinner barrier between the nanocrystal surface and water. If water reaches the nanoparticle surface, it can oxidize the nanocrystal, which decreases the emission efficiency. We have demonstrated this phenomenon by intentionally stripping off the dynamic surface exchanged nanoparticle coatings with repeated washings or dialysis, resulting in quenched fluorescence. With respect to retaining fluorescence over time, the AEE coated QDs performed with the highest emission intensity among the thin, surface-exchanged coatings, second only to the lipopolymer encapsulated QDs. While the ME coating demonstrated remarkable colloidal stability relative to its thickness, the fluorescence did not persist as the particles aged.

4.2. Amino acid and peptide-based ultrathin QD coatings

4.2.1. Cys and *N*-acyl-Cys

FCS analyses were performed to determine the relative colloidal stabilities of Cys-coated QDs compared to MPA- and MPA/AEE-coated QDs; these analyses were also conducted as a function of incubation time up to 72 h after sample preparation (Fig. 4 and Table 2). Given the size and chemical properties of Cys relative to MPA (Fig. 2), similar results were expected. Indeed, analysis of the Cys-coated QDs in 0.1 M phosphate buffer, pH 7, led to autocorrelation curves that were almost identical to those obtained for MPA (Fig. 4, $t = 10$ min) and exhibited colloidal stabilities that were similar to the MPA/AEE coated systems. In addition, up to 72 h after sample preparation the Cys-coated QDs continued to exhibit near perfect colloidal stability (Fig. 4). Overall, these samples were found to be very stable over the lifetime of our analyses.

Along with the underivatized amino acid Cys, *N*-acyl-Cys was chosen as an additional surface exchange coating. QDs coated with this particular Cys derivative were prepared and analyzed to determine their stability compared to Cys-coated QDs. These particular samples were also investigated to determine the potential contribution of the free amino terminus of Cys to the overall stability and water solubility of these samples; however, it was found that *N*-acyl-Cys led to QD samples that were not water soluble upon surface exchange, preventing their analysis by FCS. This finding suggests that additional charged amino acid moieties likely contribute to colloidal stability.

4.2.2. Xaa-Cys dipeptides

Along with the amino acid Cys, Cys in dipeptides of the general form Xaa-Cys were prepared and employed as

Table 1
Fluorescence intensity stability per nanoparticle for various hydrophilic QD coatings measured by FCS

Coating	Counts/nanoparticle		Colloidal stability
	10 min	1 week	
ME	350	40	Good
MPA	620	N/A	Moderate
MPA/AEE	600	590	Very good
Lipopolymer	950	925	Very good

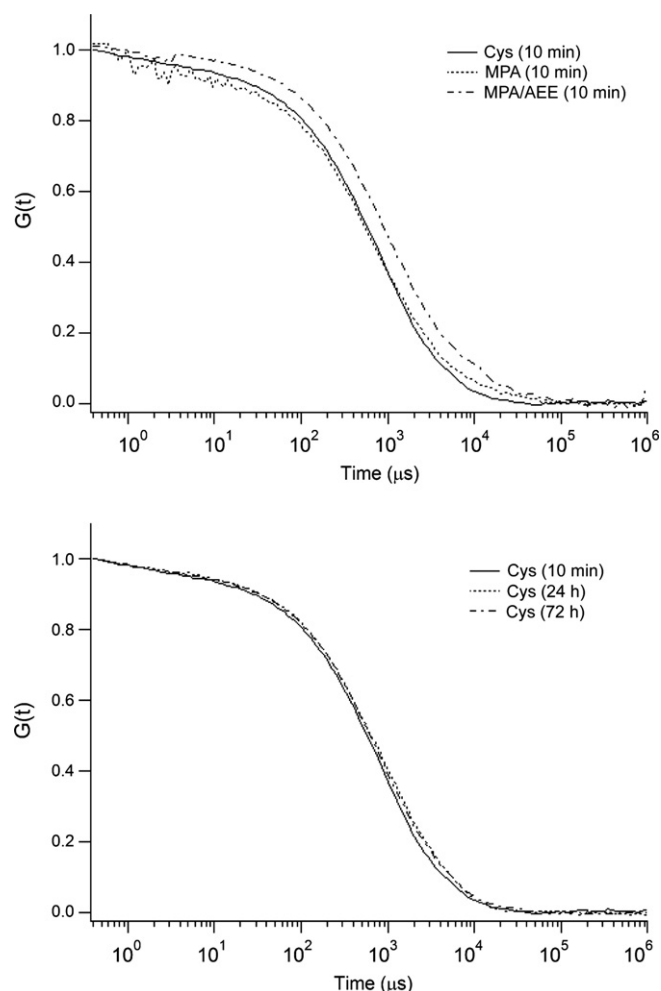


Fig. 4. FCS analyses of Cys-coated CdSe/ZnS QDs in 0.1 M phosphate buffer, pH 7. Comparison of Cys, MPA, and MPA/AEE at 10 min (upper panel); FCS analyses of Cys at 10 min, 24 h, and 72 h (lower panel).

Table 2
Fluorescence intensity stability per nanoparticle for Cys and Xaa-Cys dipeptide QD coatings measured by FCS

Coating	Counts/nanoparticle			Colloidal stability
	10 min	24 h	72 h	
Cys	160	152	148	Very good
<i>N</i> -Acyl-Cys	–	–	–	Insoluble
Gly-Cys	180	80	15	Poor
Ala-Cys	4	9	8	Poor
Ala-Cys (amide)	5	5	4	≤24 h
Asn-Cys	148	222	145	≤24 h
Asn-Cys (amide)	145	74	35	Poor
Asp-Cys	128	300	370	Very good
Asp-Cys (amide)	180	123	205	Very good
Lys-Cys	5	18	11	Poor
Lys-Cys (amide)	4	4	5	Poor
Ser-Cys	65	160	130	Very good
Ser-Cys (amide)	7	7	7	Poor

surface-exchange coatings for QDs. This series of dipeptides was generated to compare the impact of various chemical functionalities, as provided by amino acid side

chains, on the colloidal stability of their respectively coated QDs. For this analysis, six sets of dipeptides were synthesized and employed as ultrathin coatings for QDs. These dipeptides included: Gly-Cys, Asp-Cys, Asn-Cys, Ala-Cys, Lys-Cys, and Ser-Cys. For each dipeptide sequence, two samples were prepared containing either a carboxylate terminus or a carboxamide terminus, e.g., $\text{NH}_2\text{-Gly-Cys-COOH}$, “Gly-Cys” and $\text{NH}_2\text{-Gly-Cys-CONH}_2$, “Gly-Cys (amide)”. Given our findings with *N*-acyl-Cys, in all cases the dipeptides examined possessed free amino termini that should be positively charged under the conditions employed. Importantly, the amino acids chosen for inclusion in these dipeptides represent examples of amino acids that contain minimal but polar (Gly), negatively-charged (Asp), positively charged (Lys), amide (Asn), aliphatic methyl (Ala), and hydroxyl group (Ser) side chain functionalities at physiological pH values allowing a determination of their relative impact on QD colloidal stabilities to be evaluated.

Upon surface exchange with the above dipeptides, it was immediately evident that QDs exchanged with the Ala-Cys, Ala-Cys (amide), Lys-Cys, Lys-Cys (amide), and Ser-Cys (amide) dipeptides did not produce well behaved, water soluble QDs preventing their further meaningful analysis by FCS; these systems exhibited pronounced aggregation and poor colloidal stabilities. However, QDs coated with the Gly dipeptides, Asp dipeptides, Asn dipeptides and Ser-Cys led to water-soluble samples; these particular dipeptide-coated systems were compared by FCS analyses as a function of incubation time from $t = 10$ min up to 72 h after their preparation as shown in Fig. 5.

As a function of their side-chain identities, with the Gly-Cys and Gly-Cys (amide) coatings, QDs with reasonable colloidal stabilities were obtained immediately upon sample preparation ($t = 10$ min); however, upon increased incubation time ($t = 22$ h and 72 h), both Gly-Cys and Gly-Cys (amide) began to exhibit pronounced aggregation with Gly-Cys (amide) being the less stable of the two Gly-containing dipeptides; Gly-Cys (amide) became refractory to analysis at $t = 72$ h. In stark contrast, the Asp-Cys and Asp-Cys (amide) samples, containing a carboxylic acid side chain in comparison to Gly, were found to be remarkably stable over the timeframe of our analyses: both samples maintained a level of colloidal stability that was comparable to Cys alone throughout the sample incubation time as illustrated in Fig. 5. Comparable to the Asp-containing dipeptides, the Asn-containing dipeptides (which contain a side chain with a terminal amide moiety) exhibited colloidal stabilities that were initially similar to those of Cys alone and the Asp-Cys dipeptides; however, while it was observed that the Asn-Cys coated QDs remained reasonably stable and comparable to Cys alone and the Asp-containing dipeptides, the Asn-Cys (amide) coated samples exhibited significant aggregation over time (Fig. 5, middle and lower panels). Finally, unlike the behavior of Ser-Cys (amide) noted earlier, the Ser-Cys coated samples were found to be quite stable.

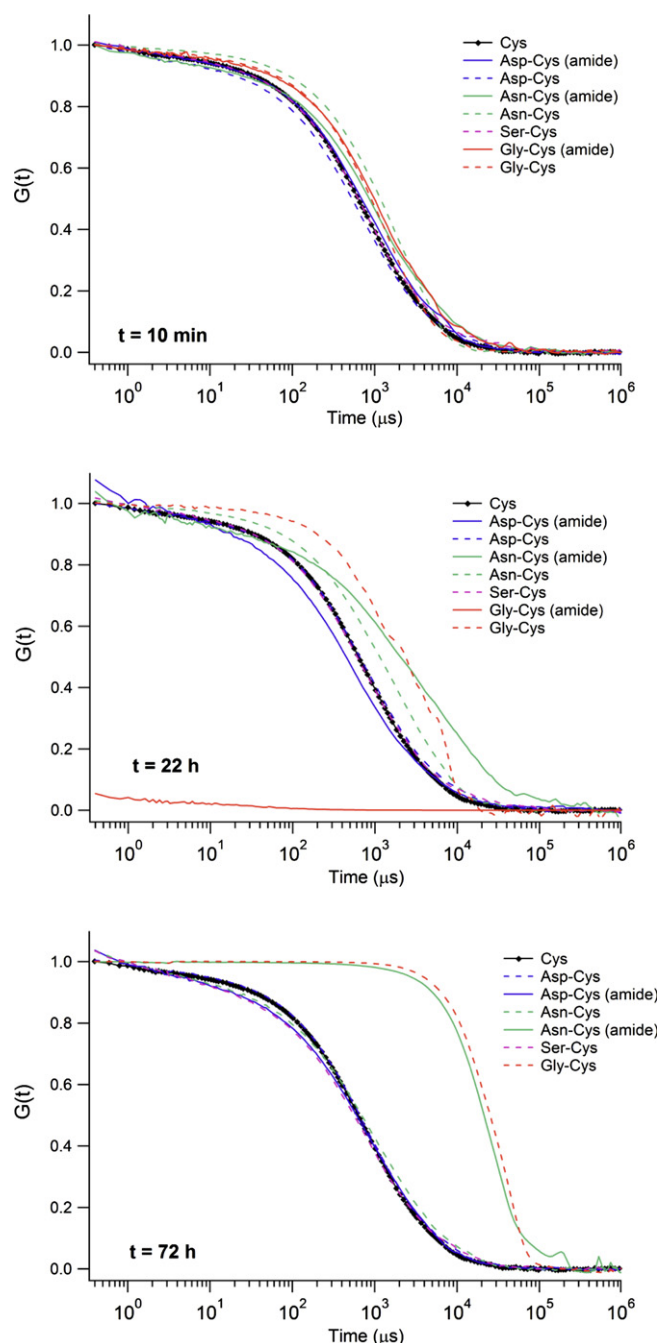


Fig. 5. FCS analysis of Xaa-Cys and Xaa-Cys (amide) dipeptide-coated CdSe/ZnS QDs in 0.1 M phosphate buffer, pH 7; incubation times upon analysis: $t = 10$ min (upper panel), 22 h (middle panel) and $t = 72$ (lower panel).

4.2.3. Emission properties

In examining these systems overall, it appears that there is a clear correlation between very good colloidal stability and high fluorescence count rates (Table 2). Dipeptide coatings leading to these attributes include Asp-Cys, Asp-Cys (amide) and Ser-Cys. Furthermore, Asn-Cys appears to be a very reasonable coating because it combines a high fluorescent count rate with moderate colloidal stability. In contrast, all dipeptide-coated samples characterized as

exhibiting poor colloidal stabilities were found to exhibit either very low fluorescence count rates similar to background from the onset [e.g., Ala-Cys, Lys-Cys, Lys-Cys (amide), and Ser-Cys (amide)] or exhibit rapidly diminishing count rates as a function of incubation time [Gly-Cys, Asn-Cys (amide)]. Finally, there are also samples that display moderate colloidal stabilities, but poor count rates [e.g., Ala-Cys (amide)].

5. Conclusions

The foregoing study has determined that CdSe/ZnS nanoparticles can be rendered water-soluble and can retain reasonable colloidal stabilities in buffered aqueous media through the use of surface-exchanged, ultrathin non-peptide and dipeptide coatings. In the case of the non-peptide coatings explored, ME, MPA, and MPA/AEE conjugated systems can attain colloidal stabilities in the good-to-very good range comparable to a lipopolymer encapsulated system studied in parallel over an extended timeframe of up to one week. While in some instances (ME and MPA) this timeframe results in a loss of fluorescence intensity, in one case (MPA/AEE) fluorescence intensity is maintained. In comparison, we also show that simple surface-exchanged coatings based on the amino acid Cys can lead to water soluble systems and promote QD colloidal stability over extended time frames; in particular, samples containing Gly and Asp within the context of an Xaa-Cys dipeptide lead to well-behaved and colloiddally-stable QDs; however it appears that in instances where a hydrophobic or positively-charged side chain is present (Ala or Lys, respectively) unstable systems are generated. Of overall importance, the above findings indicate the ability to generate extremely small (less than 10 nm), colloiddally stable nanoprobes that have the potential to function as in vivo optical imaging probes for a variety of purposes.

Acknowledgements

We gratefully acknowledge the financial support of the National Institutes of Health (R21 DK77051-01) and the IUPUI Nanoscale Imaging Center.

References

- [1] A.P. Alivisatos, W.W. Gu, C. Larabell, *Ann. Rev. Biomed. Eng.* 7 (2005) 55.
- [2] W.C.W. Chan, *Biol. Blood Marrow Transplant.* 12 (2006) 87.
- [3] C.B. Murray, D.J. Norris, M.G. Bawendi, *J. Am. Chem. Soc.* 115 (1993) 8706.
- [4] A.P. Alivisatos, *Science* 271 (1996) 933.
- [5] C. Donega, S.G. Hickey, S.F. Wuister, D. Vanmaekelbergh, A. Meijerink, *J. Phys. Chem. B* 107 (2003) 489.
- [6] Z.A. Peng, X. Peng, *J. Am. Chem. Soc.* 123 (2001) 183.
- [7] R. Cohen, L. Kronik, A. Shanzer, D. Cahen, A. Liu, Y. Rosenwaks, J.K. Lorenz, A.B. Ellis, *J. Am. Chem. Soc.* 121 (1999) 10545.
- [8] W.L. Wilson, P.F. Szajowski, L.E. Brus, *Science* 262 (1993) 1242.

- [9] W. Martienssen, H. Warlimont (Eds.), Springer Handbook of Condensed Matter and Materials Data, vol. 18, Springer Verlag, 2005, p. 1120.
- [10] W.C.W. Chan, D.J. Maxwell, X. Gao, R.E. Bailey, M. Han, S. Nie, Curr. Op. Biotechnol. 13 (2002) 40.
- [11] S.V. Kershaw, M. Harrison, A.L. Rogach, A. Kornowski, IEEE J. Sel. Top. Quantum Electron. 6 (2000) 534.
- [12] S. Kim, Y.T. Lim, E.G. Soltész, A.M. De Grand, J. Lee, A. Nakayama, J.A. Parker, T. Mihaljevic, R.G. Laurence, D.M. Dor, L.H. Cohn, M.G. Bawendi, J.V. Frangioni, Nat. Biotechnol. 22 (2004) 93.
- [13] J.G. Brennan, T. Siegrist, P.J. Carroll, S.M. Stuczynski, P. Reynnders, L.E. Brus, M.L. Steigerwald, Chem. Mater. 2 (1990) 403.
- [14] L. Qu, Z.A. Peng, X. Peng, Nano Letters 1 (2001) 333.
- [15] M.J. Murcia, D.L. Shaw, H. Woodruff, C.A. Naumann, B.Y. Young, E.C. Long, Chem. Mater. 18 (2006) 2219.
- [16] B. Ballou, B.C. Lagerholm, L.A. Ernst, M.P. Bruchez, A.S. Waggoner, Bioconj. Chem. 15 (2004) 79.
- [17] J.K. Saeeda, T. Nam, A. Khademhosseini, J. Xing, R.S. Langer, A.M. Belcher, Nano Letters 4 (2004) 1421.
- [18] H. Mattoussi, J.M. Mauro, E.R. Goldman, G.P. Anderson, V.C. Sundar, F.V. Mikulec, M.G. Bawendi, J. Am. Chem. Soc. 122 (2000) 12142.
- [19] E.R. Goldman, I.L. Medintz, A. Hayhurst, G.P. Anderson, P. George, Mauro, B. Iverson, G. Georgiou, H. Mattoussi, Anal. Chim. Acta 534 (2005) 63.
- [20] B. Dubertret, P. Skourides, D.J. Norris, V. Noireaux, A.H. Brivanlou, Science 298 (2002) 1759.
- [21] M. Xie, H.H. Liu, P. Chen, Z.L. Zhang, X.H. Wang, Z.X. Xie, Y.M. Du, B.Q. Pan, D.W. Pang, Chem. Comm. 44 (2005) 5518.
- [22] B.C. Lagerholm, M. Wang, L.A. Ernst, D.H. Ly, H. Liu, M.P. Bruchez, A.S. Waggoner, Nano Letters 4 (2004) 2019.
- [23] J.M. Harris, Poly(ethylene glycol) Chemistry, Biotechnical and Biomedical Applications, Plenum Press, New York, 1992.
- [24] S.I. Jeon, J.H. Lee, J.D. Andrade, P.G. de Gennes, J. Colloid Interface Sci. 142 (1991) 149.
- [25] Y. Ikada, Adv. Polym. Sci. 57 (1984) 104.
- [26] M. Amiji, K. Park, J. Biomater. Sci. Polym. Ed. 4 (1993) 217.
- [27] K.L. Prime, G.M. Whitesides, Science 252 (1991) 1164.
- [28] E. Ostuni, R.G. Chapman, R.E. Holmlin, S. Takayama, G.M. Whitesides, Langmuir 17 (2001) 5605.
- [29] T. McPherson, A. Kidane, I. Szleifer, K. Park, Langmuir 14 (1998) 176.
- [30] L.X. Yin, Y.Q. Wang, G.S. Pang, Y. Kolytyn, A. Gedanken, J. Colloid Interface Sci. 246 (2002) 78.
- [31] X.Y. Chen, D.P. Randall, C. Perruchot, J.F. Watts, T.E. Patten, T. von Werne, S.P. Armes, J. Colloid Interface Sci. 257 (2003) 56.
- [32] D.K. Kim, M. Mikhaylova, Y. Zhang, M. Muhammed, Chem. Mater. 15 (2003) 1617.
- [33] A.A. Guzelian, U. Banin, A.V. Kadavanich, X. Peng, A.P. Alivisatos, Appl. Phys. Lett. 69 (1996) 1432.
- [34] M.A. Hines, P. Guyot-Sionnest, J. Phys. Chem. 100 (1996) 468.
- [35] B.O. Dabbousi, V.J. Rodriguez, F.V. Mikulec, J.R. Heine, H. Mattoussi, R. Ober, K.F. Jensen, M.G. Bawendi, J. Phys. Chem. B 101 (1997) 9463.
- [36] O. Akcikir, J. Therrien, G. Belomoin, N. Barry, J.D. Muller, E. Gratton, M. Nayfeh, Appl. Phys. Lett. 76 (2000) 1857.
- [37] T. Pellegrino, L. Manna, S. Kudera, T. Liedl, D. Koktysh, A.L. Rogach, S. Keller, J. Raedler, G. Natile, W.J. Parak, Nano Letters 4 (2004) 703.
- [38] P. Zhang, L. Li, C. Dong, H. Qian, J. Ren, Anal. Chim. Acta 546 (2005) 46.
- [39] F. Pinaud, D. King, H.P. Moore, S. Weiss, J. Am. Chem. Soc. 126 (2004) 6115.
- [40] D. Magde, E.L. Elson, W.W. Webb, Phys. Rev. Lett. 29 (1972) 705.
- [41] E.L. Elson, D. Magde, Biopolymers 13 (1974) 1.
- [42] H. Qian, E.L. Elson, Appl. Opt. 30 (1991) 1185.
- [43] R. Rigler, U. Mets, J. Widengren, P. Kask, Eur. Biophys. J. 22 (1993) 169.
- [44] R. Rigler, E.S. Elson (Eds.), Fluorescence Correlation Spectroscopy: Theory and Applications, Springer, Heidelberg, 2001, p. 331.
- [45] D.V. Talapin, A.L. Rogach, A. Kornowski, M. Haase, H. Weller, Nano Letters 1 (2001) 207.
- [46] K.S. Suslick, Ultrasound: Its Chemical, Physical, and Biological Effects, VCH, New York, 1988, p. 140.
- [47] R.E. Bailey, S. Nie, J. Am. Chem. Soc. 125 (2003) 7100.
- [48] T. Ikeda, H. Hagihara, Acta Cryst. 21 (1966) 919.
- [49] W.C. Chan, S. Nie, Science 281 (1998) 2016.
- [50] S.F. Wuister, I. Swart, F. van Driel, S.G. Hickey, C. Donega, Nano Letters 3 (2003) 503.
- [51] T.U. Pons, H. Tetsuo, I.L. Medintz, H. Mattoussi, J. Phys. Chem. B 110 (2006) 20308.
- [52] T. Jankowski, R. Janka, in: R. Rigler, E.S. Elson (Eds.), Fluorescence Correlation Spectroscopy: Theory and Applications, Springer, Heidelberg, 2001.
- [53] W.C.W. Chan, D.J. Maxwell, X.H. Gao, R.E. Bailey, M.Y. Han, S.M. Nie, Curr. Opin. Biotechnol. 13 (2002) 40.